J. Cosmet. Sci., 51, 323–341 (September/October 2000)

Papers presented at the Annual Scientific Seminar of the Society of Cosmetic Chemists (Friday's Program)

May 11–12, 2000
Hilton Toronto
Toronto, Ontario

A Study on Pigment Dispersion in Color Cosmetics: Milling Process and Scale-up

Di Qu, Ph.D. and Jeffrey W. Duncan

Amway Corporation, 7575 E. Futon Street, Ada, MI 49355)

INTRODUCTION

Pigment dispersion in color cosmetics is a critical aspect which directly affects product quality and manufacturing cost. Typical pigments are supplied in powder form and contain different sizes of primary particles, aggregates, and large agglomerates that need to be adequately dispersed in final products. In addition to chemical means such as surfactants and surface coatings, mechanical means are also widely used to disperse pigment. In this study, a batch milling process using a high-speed rotor-stator mill was evaluated at two different setups, namely in-tank and in-line milling.

MATERIALS, EQUIPMENT AND METHODS

Commercially available oil and water dispersible pigments (red and black iron oxides) were used in this study. A hydrogenated jojoba oil (in colored beads form) was chosen as a model material for establishing milling process conditions due to its uniform particle size distribution. A batch is typically prepared by mixing 1% pigment or beads, 0.04% sodium lauryl ether sulfate, and 0.01% defoamer, in either an aqueous or an anhydrous medium. A Rotor-stator mill was used to mill the batch in two different processes. The first process involves milling a batch inside a tank, whereas the latter refers to recirculating through the mill outside the tank. A FBRM (focused beam reflectance measurement) in-line particle size analyzer supplied by Lasentec was used to monitor the changes in particle size and count.

RESULTS AND DISCUSSION

The pigment dispersion process was affected by several processing parameters such as rotor speed, impeller pumping capacity, batch viscosity, and recirculation flow rate. Experiments were designed to evaluate each of these parameters individually. Changes in particle count and size (mean chord length) were captured by the FBRM during milling, as shown in Figure 1. Mean particle size and the count for large particles decreased over time until they stabilized at a constant level, which indicated the effective end of the milling process. The counts for total and small particles increased as the result of milling.

A. Effect of Rotor Speed: In-Tank Milling

Rotor speed exhibited a significant effect on pigment dispersion. The higher the speed, the faster the particle size decreases. Two contributing factors are tip speed and turnover rate. Tip speed of the mill provides high shear and impingement force, which act to break down the particles. The batch turnover rate dictates how frequently the particles pass through the mill. Figure 2 shows the rate of large particle count reduction at various mill rotation speeds.

B. Effect of Recirculation Flow Rate: In-Line Milling

At constant rotor speed, the in-line milling process was primarily affected by the recirculation flow rate. Higher flow rate caused the particles to flow through the mill more frequently and therefore yielded a faster milling process, as shown in Figure 3. To achieve a 60% reduction in large particle count, the milling time was about five times longer at the flow rate of 22.3 ml/s than that at 71.2 ml/s.

C. In-Tank vs. In-Line

Figure 4 shows the performance comparison between in-tank and in-line milling processes. At the same rotor speed, in-tank milling is much more efficient than in-line milling. The result also supports the conclusion that batch milling is a flow-controlled process. The batch turnover rate is much slower for in-line milling than that of in-tank milling, resulting in a loss efficient unit operation.

D. Effect of Batch Viscosity

Since batch milling is affected by flow properties, product viscosity shows a significant effect on this process. Reduction of large particles was about 3 times faster in a lower viscosity batch, as indicated by Figure 5. This result suggests that in order to achieve the same level of pigment dispersion, longer milling time is required in higher viscosity batches.

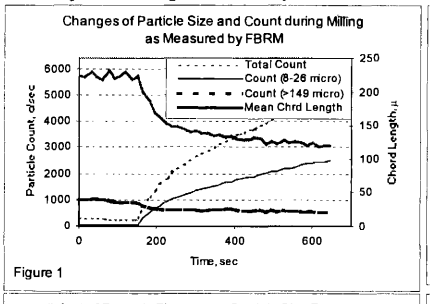

Figure 1

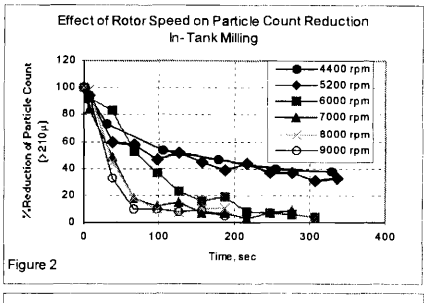

Figure 2

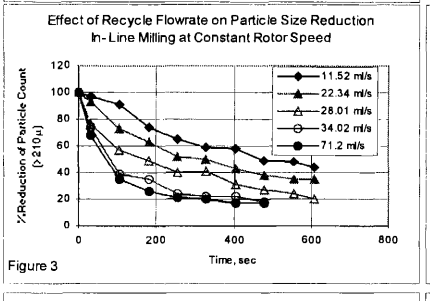

Figure 3

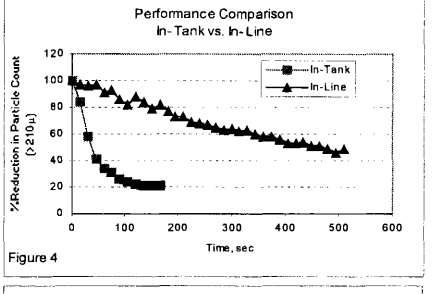

Figure 4

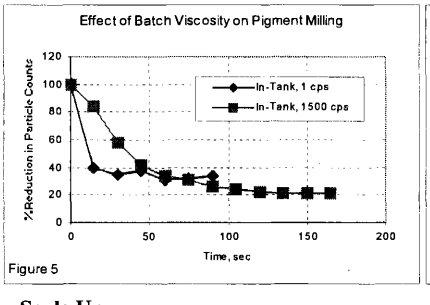

Figure 5

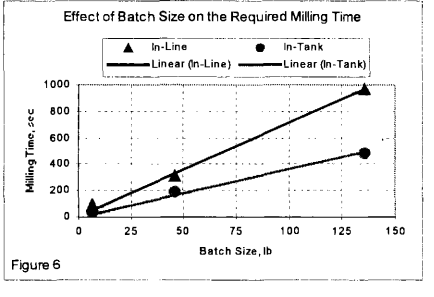

Figure 6

E. Scale Up

A series of milling tests were conducted at various sizes of pilot plant equipment. While holding mill size and speed constant, a linear function is observed between batch size and milling time for both in-tank and in-line milling processes (Figure 6). This graph indicates that the milling time required to achieve a target milling level can be predicted by using the slope of the line calculated from lab or pilot test results.

SUMMARY

The results of this study indicate that the pigment milling process is generally affected by rotor speed and by batch turnover rate. Consequently, it is affected by product viscosity, mill arrangement (in-tank or in-line), and recirculation flow rate. Higher mill speed and better batch turnover rate reduce milling time significantly. Longer milling time is required for larger batch sizes. The FBRM in-line particle analyzer is found to be a very useful tool to collect real-time data necessary for the study.

REFERENCES

1. T. Goldner, *Cosmetics & Toiletries* **101** (4): 91 – 94, 1986.
2. R. Johnson and A. Hodel, *Chemical Processing* **50** (11): 108 – 110, 1987.
3. H. Epstein, *Cosmetics & Toiletries* **110** (3): 83 – 89, 1995.
4. Lasentec, *FBRM User Manual*, Understanding & Utilizing FBRM, May 1998.

OBJECTIVE METHODS FOR MEASURING TRANSFER RESISTANCE OF VARIOUS COLOR COSMETICS

Melissa Hundey, Jesse Leverett, Bob Alexander, Terri Peterson and Ron Sharpe
Amway Corporation, 7575 E. Fulton Street, Ada, MI 49355)

INTRODUCTION:

Transfer resistance has become an important consumer-perceived characteristic in color cosmetics. However few, if any, objective methods for measuring the amount transferred have been published. Various techniques were evaluated to assess and provide an objective determination of transfer resistance. Foundations and lip-colors were screened using these techniques under different experimental conditions. Both *in vitro* and *in vivo* tests were assessed for acceptability as screening and measurement tools.

BACKGROUND:

Seventy-five percent of consumers in a recent panel felt transfer resistance to be an important characteristic in cosmetics. However, far less felt they had experienced a product that met their expectations. Most panelists felt transfer resistant cosmetics should not come off with casual contact and should last throughout the day[1]. In other words, consumers expect a product that stays where they put it. The product should not come off on their collar in the morning (when the product is freshly applied), or come off throughout the day with casual contact (after the product has been in place some time). Such expectations do not seem unreasonable. Yet, in order to meet and exceed these consumer desires, a simple screening method would be extremely useful to the cosmetic formulator.

METHODS & VARIABLES:

In vitro and *in vivo* methods were examined to evaluate transfer resistance.

An Ink Rub Tester (*Testing Machines, Inc.*, Model #10-18-01-0001) was modified to assess the transfer resistance of foundations *in vitro*. Cosmetics sponges covered with *Transpore Tape* have similar absorption to skin. Thus product would behave similarly on this substate as it does on skin. A weighed amount of product was applied and allowed to set for five to ten minutes. The mechanical arm of the instrument was equipped with a pre-weighed sponge with a texture that simulated cotton. The arm was then allowed to rub the covered surface twelve times with constant pressure. The amount of product transferred was calculated based on the increased weight of the sponge. Visual assessments and Image Analysis were used to aid in the evaluation.

In vivo testing of foundation was preformed by applying a weighed amount of product over a pre-marked area on the cheek. The test product was allowed to set a predetermined amount of time. The area was then swiped by hand five times with a pre-weighed white tissue. The amount transferred was calculated through the weight gain of the tissue. This information was then correlated to both visual assessments and Image Analysis data. Variables were reviewed.

In vivo testing of lip-color was preformed in a similar manner to the foundation testing. Pre-weighed lip-color was applied to the lips and allowed to set a predetermined amount of time. The amount of color applied was determined through the weight difference of the stick after application. Participants were then asked to "kiss" a pre-weighed tissue for five seconds. Amount transferred was again calculated through weight gain of the tissue. Visual assessments and Image Analysis were used in correlating the data. Variables were reviewed.

Variables such as color of product, pressure of removal and time product was allowed to be worn were examined.

RESULTS:

The first variable to be examined was product color. Color of *some* formulation types (i.e. most lip-colors) demonstrated a large impact on the visual amount transferred. The darker the shade the easier transferred pigment was to observe. However, it is important to note that actual weight transferred did not change due to color variations and that certain formulation types did not demonstrate this phenomena.

Pressure of rubbing was the next variable to be evaluated *in vivo*. Only light pressure was important, since simulating casual contact was the intent. A *Wagner Force 5 Capacity Gauge* (Model FDV-30) was used to determine pressure for the *in vivo* testing. Minor pressure variations (500+/-200g) did not effect percent transferred. Visual assessments and Image Analysis also correlated with these results.

Initial transfer resistance testing, which was preformed five minutes after application, was the most straightforward testing to preform on cosmetics. However this manner of testing provides limited information to the cosmetic formulator. Since long wear is also of importance to the consumer, this aspect too must be evaluated. Long-term transfer resistance has proven to be a challenge to objectively measure since the skin is not static. It is known that sebum, which develops throughout the day, can have negative consequences on makeup[2]. Currently surveys are underway to determine if short-term transfer resistance results correlate to consumers' perceptions and expectations for all day wear.

CONCLUSIONS:

Certain variables were examined in the testing. Color of product was determined to be of little importance to the amount transferred via weight. However darker shades of *some formulation types* had a direct influence on the visual perception of the transfer resistance while other did not demonstrate this phenomena. Light pressure variations during removal were also evaluated as a variable for accurate transfer measurements. This variable, surprisingly, allowed for slight changes without affecting the amount transferred immediately after application. Time was also varied in assessing the transferability throughout the day.

1. *Kintish, Lisa. Soap Cosmetics Chemical Specialties. 1998. Vol. 74, Issue. 5, pp. 32.*
2. *Aust, et al., Cosmetic Claims Substantiation. Vol. 18.*

CERAMIC MICROSPHERES

Madeline P. Shinbach

3M Company, 3M Center, St. Paul, MN 55144-1000

INTRODUCTION:

A new class of cosmetic raw materials has been engineered using ceramic technology. Ceramic spheres of high purity and excellent color are manufactured in a controlled narrow particle size range, representing a new generation of filler pigments suitable for use in a wide range of decorative cosmetics and other personal care products. The manufacture of the ceramic spheres involves a proprietary high temperature technique. The process is capable of transforming amorphous shaped inorganic particles into spheroidal forms.

As do all spherical particles, the ceramic microspheres possess excellent skin feel due to the "ball bearing" effect as they are rubbed out. The microspheres are unusual in their low oil absorption and relatively high bulk density which permits incorporation into dispersed systems at significant levels without either initial or long term viscosity increase. The particles function as an "invisible" filler useful in formulating deep shades in which the chalky whitening effect of many ingredients is a disadvantage. The inorganic microspheres offer a cost effective alternative to polymeric microparticles and are completely compatible with the full range of aqueous and non-aqueous formulations.

MATERIAL, PROCESS AND PROPERTIES OF CERAMIC MICROSPHERES:

A. Process: Particles are passed through a natural gas/air flame of approximate stoichiometric proportions with the particles reaching temperatures up to 1350°C. As the mineral particles melt, spheroidal formation occurs. The flame-formed product is cooled by mixing with ambient temperature air and then separated from the resulting gas stream with a cyclone device.

B. Materials: Materials with chemical compositions substantially consisting of the following categories – clay, talc, and hydrated silicates such as mica will be topics of discussion. The high temperature process converts the morphology from crystalline to amorphous resulting in a ceramic or glass composition. This ceramic composition of the microspheres provides its extreme chemical inertness, stability, and insolubility.

C. Properties: The transformation from an amorphous or platy shaped particle to a sphere can be expected to yield a number of interesting changes in material properties. The significant reduction in surface area achieved can be demonstrated in Fig. 1. A result of the minimized surface area can then be shown in Fig. 2 by the corresponding reduction in oil absorption by these nonporous spheres. The reduced surface area also enables increased ease of dispersibility of the microspheres as well as higher pigment loading potential due to lower viscosity buildup. The microspheres allow for an efficient packing factor leading to increased bulk densities as compared to the unspheroidized material. The spherical nature, as shown in Fig. 3, provides lower coefficient of friction values as would be expected with a "ball bearing" as opposed to a platy structure leading to an enhanced texture or "feel".

COSMETIC APPLICATIONS:

A. Pressed Powder: The performance of spheroidal magnesium silicate was evaluated in a pressed powder formulation versus a talc control. The spherical filler improved slip and imparted the perception of increased softness and creaminess. In a pressed powder eyeshadow formulation, 20% spheroidal magnesium silicate was found to yield equal or better slip and skin feel when compared to 10% boron nitride or polymethylmethacrylate (PMMA). Even at these levels, the spherical ceramic product offers an economical alternative to other texture enhancers. The nonporous nature and inertness of the spheroidal magnesium silicate are advantageous in that the texture of the formulated product remains constant over time.

B. Lipstick: In lipsticks, ceramic microspheres offer a means to incorporate significant levels of inert filler to improve adhesion to the lips as well as to reduce creeping and feathering in moisturizing formulations. Because the atmospheric and chemical water have been removed, the ceramic microspheres are more suitable for use in anhydrous, hot pour systems than native or natural (raw) minerals. 8-11% levels of spheroidal magnesium silicate were added to a transparent gloss lipstick. The result was a creamy emollient product which adhered well to the lips. Without the added filler, the texture of gloss lipsticks tends to be greasy, yet hard, due to the higher wax levels used to achieve high temperature stability. Polymeric fillers have the disadvantage of porosity which can cause the texture to become drier over time or vary according to processing conditions.

C. Powder Cream Formulation: The objective in the development of a powder cream product is to achieve the highest pigment load possible while maintaining pourability in the melted state. Ceramic microspheres, with or without surface treatment, can be used to raise the solids percentage due to their properties of low surface area, nonporosity, and low oil absorption. Other spherical materials commonly used to achieve a smooth, dry feel have the disadvantage of high oil absorption which reduces pourability of the hot melt.

Fig. 1 Reduction in Surface Area Due to Spheroidization

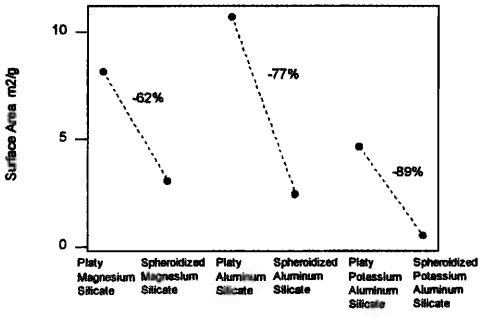

Fig. 2 Reduction in Oil Absorption Due to Spheroidization

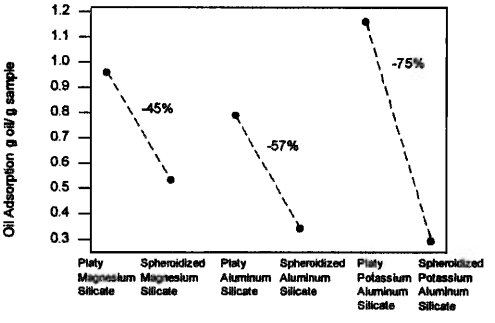

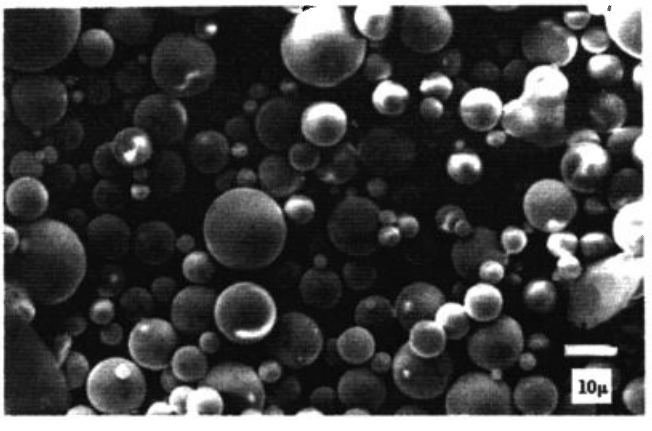

Fig. 3 Scanning Electron Micrograph of Spheroidized Potassium Aluminum Silicate

THE CONTRIBUTION OF EMOLLIENTS AND EMUSIFIERS TO SKIN EFFICACY

Johann W. Wiechers, Ph.D.
Uniqema, PO Box 2, 2800 AA Gouda, The Netherlands

Cosmetic skin care formulations without emollients or emulsifiers are hardly conceivable. Emollients have been used for centuries to impart a specific skin feel as well as for their secondary skin efficacy benefits such as skin moisturization and elasticity. Whereas the first reason for using emollients remains unchanged, the second reason is gaining importance with the current strive towards ever more efficacious cosmetic products.

For this reason, we measured many personal care ingredients for their performance towards three skin effects: moisturization, elasticity and substantivity. Non-formulated emollient was applied to the skin and left for a time up till 6 hours after which the product was removed (moisturization and elasticity) and the effect measured by non-invasive skin bioengineering techniques. This revealed that these emollients had a wide range of efficacy towards these activities. Their performance was expressed relative to untreated skin (0%) and a benchmark product-treated skin (100%). Using artificial cut-off values at 30 and 70%, this relative performance testing allowed the identification of low (>30%), medium (30-70%) and high performing (>70%) ingredients (see Figure 1). When the performances in the various skin activities were plotted against each other, it could be concluded that these personal care ingredients were specific in their skin efficacy, *i.e.* they may be good in one property but poor in another. Figure 2 shows that the emollients could be subdivided in two groups, one group of ingredients with a low elasticity performance but a wide range of moisturization performances and another category of emollients with a low moisturization performance but a wide range of elasticity performances. Subsequent work in which combinations of low- and high-performing moisturizing emollients were incorporated in formulations indicated that the efficacy of the formulation changed linearly as a function of the concentration of high-performing emollient, provided a certain threshold value had been reached (see Figure 3). The same could be observed for elasticity and substantivity.

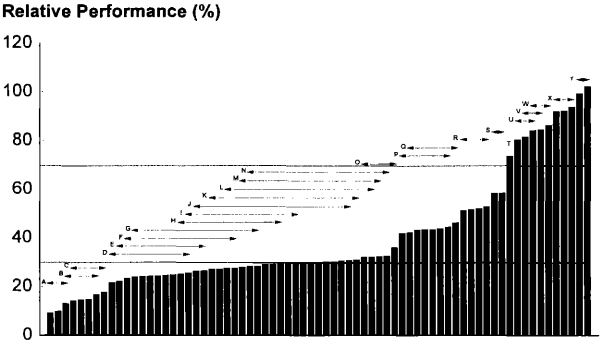

Figure 1 *Moisturization performance of non-formulated personal care ingredients six hours after application relative to untreated (0%) and glycerine-treated skin (100%).*

Unfortunately, it was not possible to measure the relative efficacy performance of pure emulsifiers in the same way as we tested the emollients as they cannot be applied to the skin in an undiluted form. When you formulate them, the other ingredients are likely to contribute to the skin performance as well. We therefore used the previously tested formulation series as the base formulation for the emulsifier studies. Using only the low- and high-performing emollient containing formulations, we changed the emulsifier whilst keeping the rest of the formulations constant. All emulsifiers were used at realistic concentrations. In addition,

glycerine was added to two emulsifier systems to investigate the addition effect that this important humectant could have on the skin efficacies studied. Experimental conditions were identical to the previous studies.

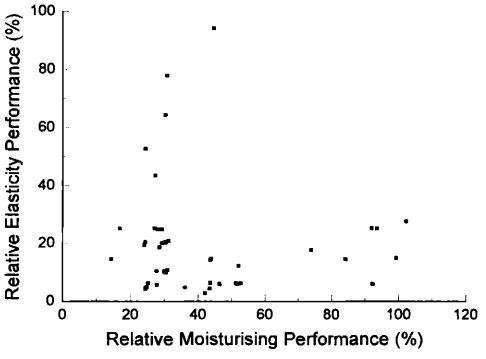

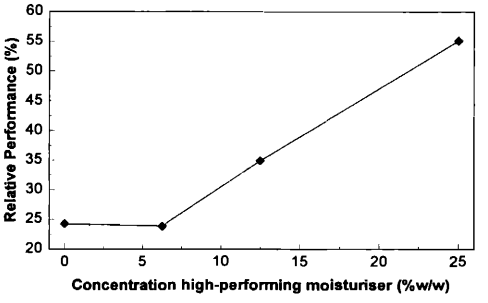

Figure 2 *Relative elasticity performance of non-formulated personal care ingredients as function of their relative moisturization performance*

Figure 3 *Relative moisturization performance of formulations as function of the concentration of high-performing moisturizers*

For all skin benefits, the most important contributor to the overall efficacy of the formulation was the performance of the emollient. Formulations containing the high-performing emollient (B) always demonstrated a higher skin efficacy than the formulations containing the low-performing emollient (A), independent of the nature of the emulsifier system (#1-9) (see Figure 4). This was in line with the previous formulation study as the relative performances of the selected low- and high-performing emollients were very different. Much more surprising was the fact that certain emulsifiers were capable of improving the skin efficacy of formulations, regardless whether low- or high-performing emollients were used. This was independent of the skin efficacy studied, meaning that the emollient efficacy enhancing (EEE) effect of the emulsifier (system) was independent of the type of efficacy studied. Within the range of emulsifier systems studied, the w/o-emulsifier systems had both the highest and the lowest EEE. It can therefore not be attributed to the type of emulsifier. The addition of glycerine to formulations was only useful for those systems where either the emollient or the emulsifier or both were not optimal for delivering the skin efficacy. However, in formulations already containing the optimal combination of emollient and emulsifier, glycerine did not exert any further benefit for any of the skin efficacies studied.

These studies showed that the emollient decides which skin efficacy a formulation may have, but that the extent of the efficacy is determined by the combination of emollient and emulsifier.

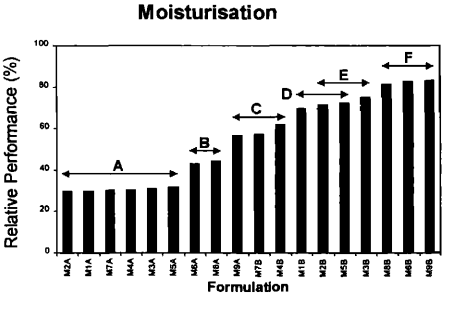

Figure 4 *Moisturization performance of eighteen moisturising formulations tested after a 6 hours application time, relative to untreated skin (0%) and glycerine-treated skin (100%).*

ANALYSIS OF THE STABILITY OF THE PRESERVATIVE, BRONOPOL, AND IDENTIFICATION OF ITS DECOMPOSITION PRODUCTS

Asira Ostrovskaya, Peter A. Landa, Anthony D. Rosalia and Daniel Maes

Estee Lauder Inc., Research and Development Center, 125 Pinelawn Road, Melville, NY 11747

Introduction: Bronopol (2-bromo-2-nitropropane-1,3-diol) has broad-spectrum anti-bacterial activity and is, therefore, used as a preservative in many toiletries, pharmaceuticals, household items and cosmetics (1). Despite its common usage, the stability of bronopol has been suspect and of great concern to the industry as a whole, because of its stability issues in products under certain conditions (2). In order to stabilize bronopol in products, we investigated the kinetics and decomposition pathways of bronopol. We further compared degradation patterns of bronopol in aqueous and methanolic solutions.

The decomposition products of bronopol have been previously postulated and examined by UV spectrophotometry, NMR, and HPLC (3-5). However, to fully identify and confirm bronopol's decomposition products we employed Gas Chromatography - Mass Spectroscopy (GC-MS). This led us to a better understanding of the degradation products, and to confirm the postulated mechanisms of bronopol's decomposition.

Methods: The stability of bronopol was investigated by High Performance Liquid Chromatography in aqueous and methanolic solutions at concentrations of 0.04g/250mL. The method employs an Inertsil ODS-2 column with a mobile phase of acetonitrile and water at 220nm.

The decomposition products of bronopol, were determined and identified via Gas Chromatography - Mass Spectroscopy (GC-MS) using a DB-1 column. This method uses an oven temperature program consisting of 40°C for 10 minutes, 5°C/min to 280°C, hold for 2 minutes. The MS collected masses 40-550 AMU at 1.4 scans/sec and data were subsequently analyzed and interpreted.

Results and Discussions:

HPLC: The kinetics of bronopol were studied at room and elevated temperatures in both aqueous and methanolic solutions. In aqueous solutions at room temperature, Bronopol degraded readily due to hydrolysis, and when solutions were heated the rate of decomposition increased. In methanolic solutions no apparent decomposition was observed even at elevated temperatures. The HPLC method is limited to the determination of bronopol levels in solutions but is not useful for determining by-products of bronopol degradation.

GC-MS: To identify the decomposition products of Bronopol and determine its degradation pathways, GC-MS was employed. GC-MS chromatograms obtained for both aqueous and methanolic solutions of bronopol, initially contained one major and one minor peak. The major peak was identified as bronopol. The mass spectrum for the minor peak was identified as 2-bromo-2-nitroethanol, previously described in the literature as result of a retroaldol decomposition of bronopol (1).

Mass Spectrum of Minor Peak at 14.9min – Identified as 2-bromo-2-nitroethanol

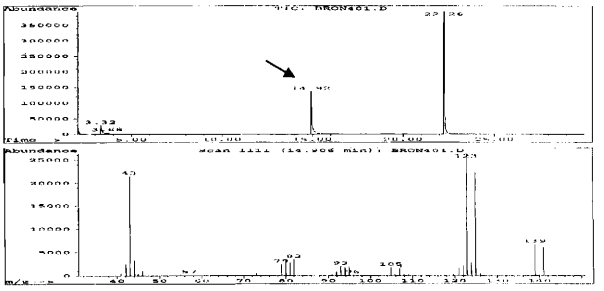

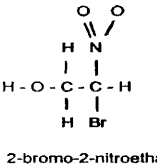

2-bromo-2-nitroethanol

Over time, two additional peaks at 3.3 and 3.7 minutes were observed and were more prevalent in aqueous solutions. The mass spectra of these two peaks were interpreted and identified as bromo-nitro-methane and 1-bromo-1-nitro-ethene, respectively (see below). These secondary peaks occur as a result of further decomposition of the intermediate, 2-bromo-2-nitroethanol.

Mass Spectra of Two Secondary Peaks

bromo-nitro-methane @ 3.3min *1-bromo-1-nitro-ethene @ 3.7min*

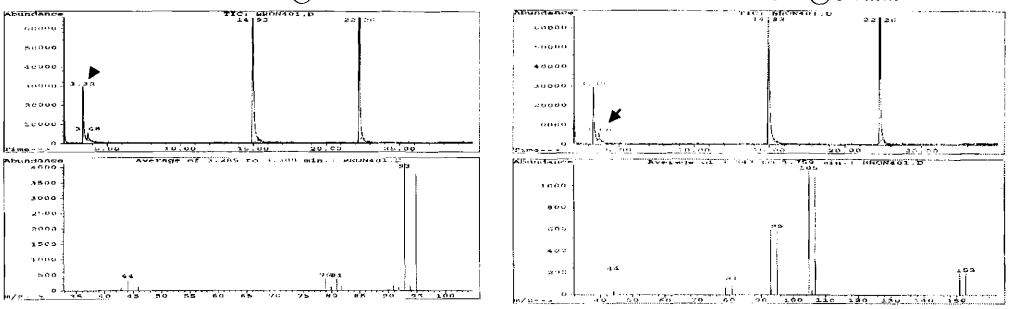

Bronopol, therefore, loses a formaldehyde molecule degrading to 2-bromo-2-nitro-ethanol. In turn, 2-bromo-2-nitro-ethanol further degrades by either one of following two pathways: 1) loss of an additional formaldehyde becoming bromo-nitro-methane or 2) loss of the hydroxyl group with the formation of a double bond between carbons becoming 1-bromo-1-nitro-ethene.

Bronopol's Initial and Secondary Decomposition Pathways in Aqueous Media

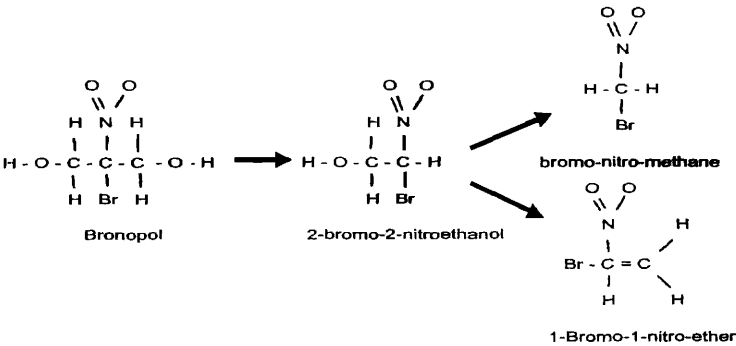

In methanol, on the other hand, the decomposition is initiated when the lone electron pair of oxygen withdraws a hydrogen from bronopol's hydroxy group. Area ratios between these two peaks indicate that the kinetics of the retroaldol mechanism in aqueous solutions is more advantageous than the decomposition mechanism in methanolic solutions.

Conclusions: By utilizing the GC-MS, we were able to identify and confirm the decomposition products of bronopol, and postulate its decomposition pathways. We were able to correlate the GC-MS data with the HPLC assay results.

We found that the primary degradation mechanism of Bronopol to 2-bromo-2-nitro-ethanol occurs readily in water and is less energetically favorable in methanolic solutions.

The subsequent degradation to bromo-nitro-methane and 1-bromo-1-nitro-ethene in methanol is found at a much slower rate due to the lower availability of the intermediate, 2-bromo-2-nitro-ethanol, in solution.

This study will allow us to collaborate with formulators to implement conditions that can improve the stability of bronopol in cosmetic formulations.

1. Kabara, J.J., *"Cosmetic and Drug Preservation,"* **1**, Marcel Dekker, Inc., New York, 31-62, *1984.*
2. Moore, K.E. and Stretton, R.J., *J. Applied Bacteriology*, **51**, 483-494, *1981.*
3. Sanyal, A.K. et. al., *J. Pharm. Biomed. Anal.*, **14**, 1447-1453, *1996.*
4. Challis, B.C. and Yousaf, T.I., *J. Chem. Soc. Perkin Trans.*, **2**, 283-286, *1991.*
5. Lian, H.Z. et. al., *J. Pharm. Biomed. Anal.*, **15**, 667-671, *1997.*

CORRELATION OF AFM/LFM WITH COMBING FORCES OF HUMAN HAIR

Roger L. McMullen*[1], Stephen P. Kelty[1] and Janusz Jachowicz*

[1]Department of Chemistry, Seton Hall University, South Orange, NJ,
*and *International Specialty Products, Wayne, NJ,*

Introduction

Scanning Probe Microscopy (SPM) is a class of techniques used to study the surface properties of materials from the atomic to micron scale. Atomic Force Microscopy (AFM) and Lateral Force Microscopy (LFM) fall under the SPM umbrella of techniques. In both these techniques, a sharp tip stylus is placed in contact with a surface to be investigated. In AFM, one obtains a topographical image by measuring the deflection of a soft cantilever, to which the tip is attached, as the tip is rastered over the surface. The cantilever deflections normal to the surface are representative of topographical surface features. In LFM, one measures the torsional twisting of the cantilever as it is rastered over the surface. These lateral cantilever deflections result from drag forces between the tip and sample surface.

Although several AFM investigations on human hair fibers have recently appeared in the literature, to our knowledge, complementary LFM studies have not been forthcoming. However, there has been a limited amount of information reported concerning the LFM of wool fibers in which different frictional domains were observed [1]. Within the realm of human hair fiber investigations, a considerable amount of interest has focused on quantifying the cuticle step heights [2,3], and characterizing the surface roughness of the morphological components of the cuticle, i.e. the exocuticle, endocuticle, and the A-layer [3]. Additionally, these studies have demonstrated the use of AFM to study hair at various degrees of hydration [1-4] and at a range of pH levels [4,5]. Other studies, primarily interested in the adsorption of cationic polymers onto hair, have also been completed [6-9]. Most recently, Parbhu *et. al.* used force-volume and nano-indentation techniques to measure the hardness and relative elastic moduli of the morphological components of the wool fiber [10]. Their results were in agreement with what one would expect considering the chemical composition of the various components of the wool fiber.

We herein report combined AFM and LFM investigations of hair fibers as an analytical tool to correlate the wet combing force (obtained using a Miniature Tensile Tester) for bulk fibers. A comparison is made using both the surface topography (AFM) and the frictional force (LFM) obtained for a single fiber with the bulk fiber assembly. Hair that has been weathered (irradiation), chemically treated (bleached, permanent waved, or dyed), or thermally exposed (curling iron or hair dryer) experiences an increase in wet combing forces. Spatially Resolved Combing Analysis allowed us to observe an increase in inter-fiber friction, in the area of the hair tress, where the damaging treatment was administered.

Methods & Results

AFM and LFM studies were performed using an AutoProbe™ CP manufactured by Park Scientific Instruments. An AFM/LFM probe head was used in conjunction with a 100 μm piezoelectric scanner, operating in the contact mode. Commercial gold-coated Si_3N_4 cantilevers with pyramidal tips (microlevers) were used in the analysis . Hair fibers were mounted to steel sample studs using epoxy or nail polish. All data sets were collected in the contact imaging mode. During each scan, images were obtained for the topographic, error signal, left-to-right LFM, and right-to-left LFM measurements simultaneously. Subsequent data analysis was performed using Image Tool 2.0 (University of Texas Health Science Center in San Antonio). All image data presented in this report is raw and otherwise unfiltered. In normal operation, the difference between actual cantilever deflection and a reference setpoint is supplied to a feedback loop connected to the z-drive (height) of the scanner. The voltage supplied to the z-drive is the origin of the topographic image data and is sensitive to topographic surface features. The error signal image reflects the difference between the actual cantilever deflection and the setpoint and is highly sensitive to changes in height. Consequently, we find that it is useful to monitor both the topographic and error signal simultaneously since they are complementary techniques. LFM data were

obtained in both scan directions providing us with two complementary images illustrating the torsional bending experienced by the cantilever in the left-to-right and right-to-left scan directions.

Combing measurements of hair tresses were performed using a Miniature Tensile Tester (Dia-Stron Ltd.) operated by MTTWIN 4.1a software. Oriental human hair (International Hair Importers & Products, Inc.) was used for all investigations due to its high radius of curvature as compared to other hair types, which are more elliptical in shape. Virgin hair, as supplied by the distributor, was compared with hair that was extracted with a series of solvents. The effect of solvent extraction on hair was investigated first by extraction with *t*-butanol and n-hexane, each for 4 hours, then with a mixture of chloroform/methanol (70:30 v/v) for 6 hours. For each extraction procedure, 3 g of hair was extracted with 250 mL of solvent. Additionally, we examined the effect of bleaching hair by using a commercial bleaching system consisting of Clairol Professional BW 2 bleaching powder and Emiliani Professional 20 Volume clear developer.

In an attempt to correlate data obtained from a miniature tensile tester with AFM/LFM data, we will present the combing analysis of untreated hair and hair that has undergone the treatment protocols described above. We will also discuss the image analysis of data obtained from AFM/LFM. For demonstration, topographic, error signal, LFM (left-to-right), and LFM (right-to-left) images have been included in Figures 1-4, respectively. These images were obtained simultaneously for a 20 μm^2 scan area on untreated hair. The scale in Figure 1 correlates darkly colored areas with lower topography and lightly colored areas with regions of higher topography. The error signal does not provide us with useful topographic information, however it does offer informative boundary data, which can be used to determine the size of features in the xy plane. The LFM data, included in Figures 3 and 4, demonstrate the torsional bending of the cantilever as it rasters across the sample in both directions. It is important to note that what appears dark in Figure 3, transpires as light in Figure 4 and vice-versa. In Figure 3 (left-to-right) dark represents areas that are higher in friction whereas light is indicative of lower frictional regions. The opposite is true for Figure 4 (right-to-left), in which light corresponds to high friction and dark represents low friction. By taking the difference between Figures 3 and 4, one can obtain relative frictional information about a particular material. However, the images must be collected at various normal forces in order to obtain a plot of torsional cantilever deflection as a function of the set point. In this study we compare virgin with solvent-extracted and bleached hair. Figure 5 provides preliminary data for each of these hair types in which the difference in the left-to-right and right-to-left LFM signals are plotted as a function of the normal force applied by the probe. The slope for each hair type, which is related to the frictional coefficient between the probe and a given hair surface, is reported in the Figure and demonstrates a larger slope for bleached and solvent extracted hair than for virgin hair. For bleachd hair, such a result is in agreement with evaluation of mechanical combing forces which suggest higher dry combing works as compared to virgin hair.

(1) Phillips, T. L.; Horr, T. J.; Huson, M. G.; Turner, P. S. *Textile Res. J.* **1995**, *65*, 445-453.
(2) Smith, J. R. *J. Microscopy* **1998**, *191*, 223-228.
(3) Smith, J. R. *J. Soc. Cosmet. Chem.* **1997**, *48*, 199-208.
(4) O'Connor, S. D.; Komisarek, K. L.; Baldeschwieler, J. D. *J. Invest. Dermatol.* **1995**, *105*, 96-99.
(5) You, H.; Yu, L. *Scanning* **1997**, *19*, 431-437.
(6) Goddard, E. D.; Schmitt, R. L. *Cosmet. & Toil.* **1994**, *109*, 55-61.
(7) Schmitt, R. L.; Goddard, E. D. *Cosmet. & Toil.* **1994**, *109*, 83-93.
(8) Hössel, P.; Sander, R.; Schrepp, W. *Cosmet. & Toil.* **1996**, *111*, 57-65.
(9) Pfau, A.; Hössel, P.; Vogt, S.; Sander, R.; Schrepp, W. *Macromol. Symp.* **1997**, *126*, 241-252.
(10) Parbhu, A. N.; Bryson, W. G.; Lal, R. *Biochemistry* **1999**, *38*, 11755-11761.

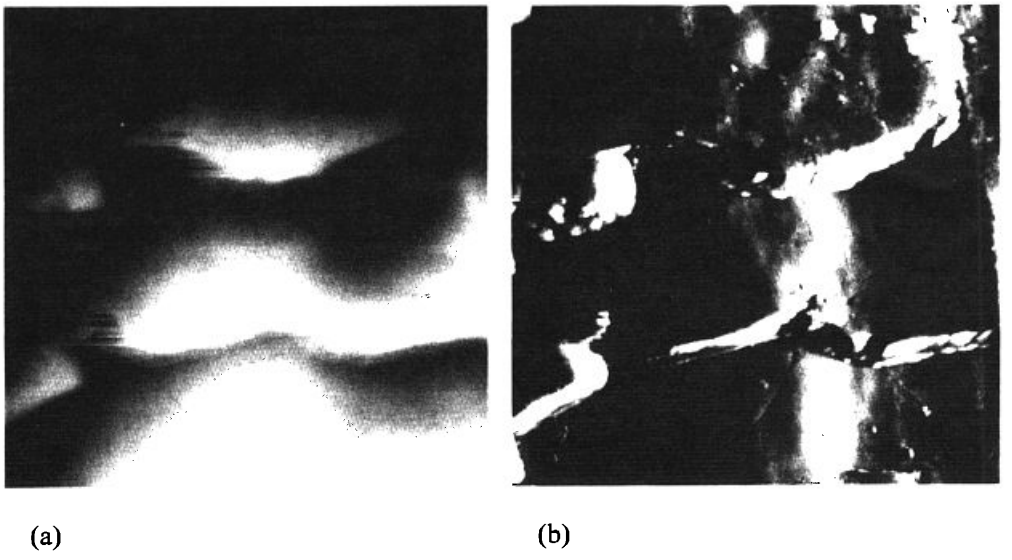

(a) (b)

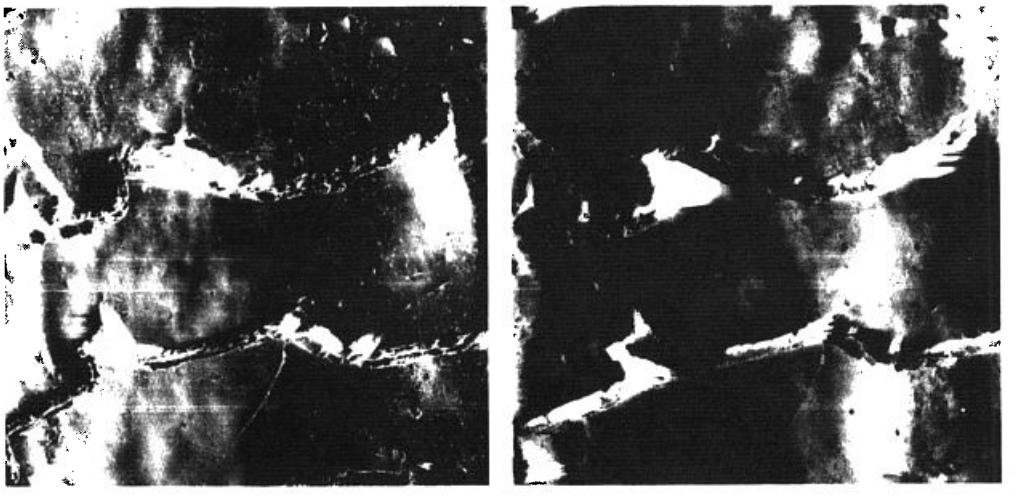

(c) (d)

Figure 1. Topography (a), error signal (b), LFM [left-to-right] (c), LFM [right-to-left] (d) for untreated hair. Images were obtained simultaneously for a 20 μm^2 scan area.

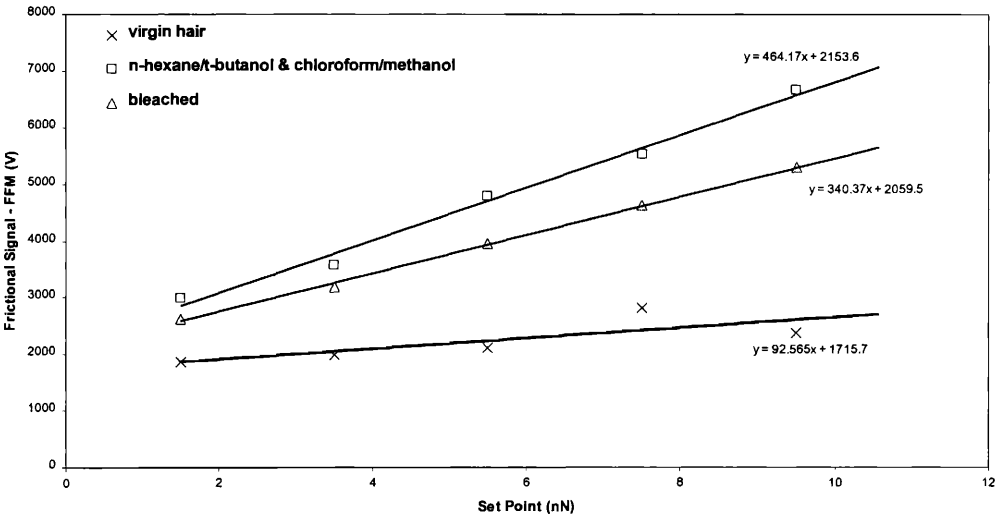

Figure 2. Frictional signal (calculated as difference between LFM left-to-right and LFM right-to-left) as a function of normal force for different types of hair.

NOVEL BOTANICAL SKIN ANTI-IRRITANTS DISCOVERED BY HET-CAM ASSAY

Danielle Simonot, Tracy Wilson and Warren Steck

Fytochem Products Inc., 110 Research Drive, Saskatoon, SK S7N 3R3 Canada

Introduction to the HET-CAM (Hen's egg test – chorioallantoic membrane)

The HET-CAM has been used as a toxicological and pharmacological model for many years[4] and has been established and proven to be a robust test with good predictive value of irritation potential[1]. In the progressing scientific movement to replace animal testing in lieu of more humane techniques, the HET-CAM allows for ethical, non-animal screening of irritating compounds and has become a common and validated technique. While the HET-CAM has traditionally been utilized to measure the irritating potential of substances, its methods have been modified to assess the anti-irritancy activity of compounds as well.

The HET-CAM involves the observation of vascular injury to the extra-embryonic chorioallantoic membrane (CAM) of 10-day old fertilized hen's eggs upon application of a substance of study. Eggs up to 10 days of age are still largely considered foodstuff[2] therefore their utilization does not conflict with legal or ethical issues, particularly animal protection laws. Further, while the CAM is a complete and living tissue, it lacks sensory innervation[3] therefore is regarded as insensitive to pain[4] and suitable for the testing of irritants. The HET-CAM incorporates aspects of both *in vitro* and *in vivo* test systems. Its *in vivo* component involves the utilization of a living, highly vascularized and metabolically-active membrane which can thereby provide an accurate depiction of the test substance on living tissue. However, it also provides several advantages of *in vitro* test methods including simplicity, rapidity, sensitivity, ease of performance and relative cheapness[5].

Based on the technique described by Dannhardt et al. (1996)[4], testing is also being accomplished by injection of test substances directly into the egg albumen. This permits prolonged incubation of samples for up to six hours, a feat not possible with the traditional HET-CAM procedure which exposes the CAM membrane upon application of the test substance and thus restricts the amount of time the membrane may remain exposed and unperturbed. This method also allows the testing of substances which may not be normally absorbed into the CAM.

Modifying the HET-CAM to assess anti-irritancy

Anti-irritant activity of an aqueous plant extract can be measured by the delay of the typical landmark irritation phenomena following the application of a standard irritant: hemorrhage, lysis and coagulation. This method has permitted the screening and identification of aqueous plant extracts which possess anti-irritating properties. Skin patch testing has confirmed this activity in at least one plant extract identified by this assay thus far.

Materials & Methods

Fresh, fertile, White Leghorn hen's eggs are incubated for a period of ten days at a temperature of 37°C with periodic rotation. Eggs are placed with the blunt end up to correctly position the airsac above the CAM. On the 10th day of incubation, the eggs are candled and their airsac delineated by pencil. Infertile eggs or those with non-viable embryos, clearly distinguishable by the lack of embryo movement or abnormalities in blood vessel development, are discarded by freezing. All eggs are then weighed and only those between 50-60 g utilized in order to maintain a standard and uniform testing criteria. Testing is carried out in a sterile, horizontal flow hood and by methodology described by Spielmann[5].

To expose the CAM for testing, the eggshell is cut away around the previously delineated line by a Dremel tool with a small cutting disk attached to the flexible head. The eggshell cap is removed by tissue forceps and the visible outer shell membrane is moistened with 0.9% isotonic NaCl solution and incubated for five minutes to soften the membrane. The NaCl solution, along with all samples and standard irritants to be utilized in the assay, are kept heated to physiological temperature in a water bath. Once the NaCl solution is wicked off and the shell membrane is carefully removed by blunt forceps, the exposed CAM is examined for any damage or abnormalities, either of which will result in its ejection from the assay.

Aqueous plant extract is carefully applied to the CAM by pipette which is then covered by plastic wrapping to keep the membrane moist, and the egg is placed in the incubator for a period of 20 minutes. Each plant extract is tested by three replicates. Following incubation, 15% lactic acid (LA), the standard

irritant, is applied to the CAM. The time taken for the three irritation phenoma (hemorrhage, lysis and coagulation) to occur up to a maximum of 5 minutes is then recorded. Following this observation, the egg is destroyed by freezing. Prior to each assay trial, two eggs are also tested with standard irritant (15% LA or 1% SDS) to provide a basal measure of standard irritation.

Measuring The Irritation Phenomena

Irritation of the CAM is gauged by the appearance of three landmark irritation phenomena (as described by Steiling[1]): hemorrhage (H), observed as bleeding out from blood vessels; lysis (L), indicated by the disappearance of small blood vessels on the CAM as a consequence either of bleeding, dystonia of these fine vessels or disintegration; and coagulation (C), either intravascular (thrombosis) or extravascular which tends to increase the CAM opacity. The irritation score (IS) of a substance, described by Speilmann[5], is then determined by the following formula:

$$IS = [(301\text{-}H)/300]5 + [(301\text{-}L)/300]7 + [(301\text{-}C)/300]9$$

The application of a standard irritant determines the basal time required for these phenoma to occur. Following the application of a plant extract to the CAM, anti-irritancy can be determined by the ability to delay the occurrence of these phenoma following application of the standard irritant.

Results & Discussion

Of a multitude of plant extracts tested, a select few were identified which showed anti-irritant properties illustrated by a significant reduction in the IS score and confirmed by human skin patch testing. Two of these plants are from the same botanical family. Subsequent isolation and testing of the plant active showed an even further reduction of irritation phenomena. Additionally, it was found that by utilization of the injection method, the longer the incubation time, the increased the effect.

At present, the Draize rabbit eye test is the only method accepted worldwide for registration of new chemicals into the marketplace[1]. Alternatives to this method have actively been sought out for the last few decades and one of the most successful assays evaluated so far has been the HET-CAM, the hen's egg-test on the chorioallantoic membrane of fresh, fertilized eggs. The HET-CAM has provided a convenient, reliable, mechanism-independent screening assay for anti-irritant action of natural substances.

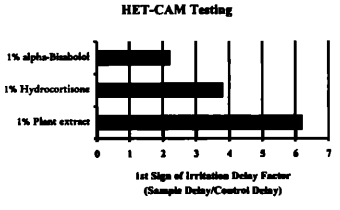

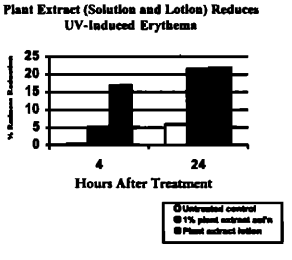

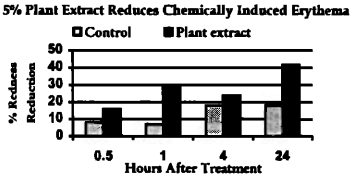

An aqueous plant extract with promising anti-irritant activity, as identified by the HET-CAM, and 1% hydrocortisone were tested competitively in a 24-hour human patch test employing 15% lactic acid as irritant. In this test the extract gave better short-term remediation of the symptoms or symptoms than was obtained with the steroid. During another human skin test, the extract was also found to reduce the effects of UV-induced erythema. Therefore, the HET-CAM has been shown to have potential as a screening tool for anti-irritant plant extracts.

1 – Steiling W., Bracher M., Courtellemont P. & de Silva O. 1999. *Toxicology in Vitro* **13**: 375-384.
2 – Bagley D.M., Waters D. & Kong B.M. 1994. *Fd Chem.k Toxic.* **32(12)**: 1155-1160.
3 – Leighton J., Nassauer J. & Tchao R. 1985. Fd Chem. Toxic. **23(2)**: 293-298.
4 – Dannhardt G., Kreher M., Nowe U. & Pies A. 1996. *Arch. Pharm. Pharm. Med. Chem.* **329**: 301-310.
5 – Spielmann H. 1995. In: O'Hare S. & Atterwill C.K. (eds) Methods in Molecular Biology Vol.43: In Vitro Toxicity Testing Protocols. Humana Press Inc., Totowa NJ

CONCENTRATION DEPENDANCE OF CRITICAL STRESS MAY BE UTILIZED TO CHARACTERIZE GELS

J. Mendoza[1],[2] MS and M. Serpil Kislalioglu[1], Ph.d.

[1]Cosmetics and Personal Care Products Technology Program, College of Pharmacy, The University of Rhode Island, Kingston, RI 02881 and

[2]Chemex Chemical Manufacturing and Exporting Co., PO Box 1448, Tegucigapa, Honduras, C.A.

INTRODUCTION

In order to define concentration dependent rheological parameters, Bentonite RV®, sodium carboxy methyl cellulose, methyl cellulose (Methocel A4C®), hydroxypropyl methyl cellulose (Methocel KM4®), pectin USP-100, Carbopol 971 NF®, RLV®(lambda), VV11PF® (iota) and VV71P® (kappa), carrageenans, guar gum U-NF and Water Lock (starch/acrylates/acryamide copolymers) A-100®, A-180®, DD-223® and G-400® were studied with oscillatory viscometry at nondestructive and destructive modes. The elastic (G'), viscous (G") and complex moduli (G*), complex viscosity (η^*), strain (γ) and the phase angles (α) were measured at the linear region where G' is independent of the shear stress. Critical stress (σ_c) at (G') and (G") were also determined from the instruments output.

EXPERIMENTAL

Preparation of the gels: The gels, with exception of Carbopol 971®, were prepared by adding sterilized distilled water to the polymer powder to obtain the pre-selected (w/w) concentration. The mixtures were left for swelling for 24 hours. They were homogenized using a Fisher Scientific (Pittsburgh, PA) Dyna-mix stirrer at 1000 rpm for 1 hr. Carbopol 971® was prepared with 1N NaOH neutralization. The concentrations used varied from 0.3% to 7.0% with no less than a 3 fold increment for each range. Five different concentrations per gel were used.

Rheological measurements: The measurements were taken within 24-48 hours of preparation. The rheological behavior of the gels was characterized at each concentration using a Bohlin Instruments Rheometer Model CVO. A stainless steel, plate and plate spindle (number 4) with 1 mm gap was used at a strain range of 0.00075 - 15 mm and frequency of 0.05 Hz. Measurements were taken at 25 °C.

RESULTS AND DISCUSSION

Description and comparison of flow properties of the gels: The gel strengths varied from 0.001Pa to 7,600 Pa. The flow types were both shear thinning and shear thickening. With increasing stress, the G" of sodium carboxy methylcellulose, methylcellulose, pectin and guar gum decreased, whereas G" of Carbopol 971® increased. The elastic nature of Carbopol 971® was also obvious from low α (10°) at all concentrations studied (0.5 - 5.0%). Pectin demonstrated a gradual decline in G' that is characteristic of a low molecular weight polymer with a broad molecular weight distribution.

The degree of sulfate esterification influences the viscoelastic properties of carrageenans. At the same concentration, the α of iota carrageenan was almost 90°. It has a lesser degree of esterification than lambda carrageenan. Kappa carrageenan, having the least degree of esterification, demonstrated purely viscoelastic behavior at 1% concentration. Its α is around 20°. Water Locks form solid gels with high degree of G' which was in the order of 500 - 1000 Pa at 1% concentrations. With exception of Water Lock A-180®, they showed an increment in G" with increased stress, denoting dilatant behavior.

Identification of concentration dependent rheological parameters: The linear, exponential, logarithmic and power equations were tested as models to seek a relationship between the (G'), (G"), (η^*), (G*), (γ) and (α) at the linear region and (σ_c) at (G') and (G") respectively, and concentration. The only parameter that provided a relationship with concentration in the gels studied was the σ_c at (G') which can be written as ($\sigma_c = \alpha + s.\ C$), where s is called the sensitivity index, Table I. The sensitivity indices given in Table I can be further categorized into three groups: In gels where $s \geq 10$, the internal elasticity increases greatly with small increments in concentration. In gels with s=1-10, the concentration moderately influences internal elasticity. The gels with $s \geq 0.01$-0.9 poorly respond to concentration changes. Sensitivity index may be useful for quick evaluation of the gels based on their concentration. The model proposed was applicable to gels of different chemical structures, molecular weights, molecular weight distributions, chain structures and viscosity types; therefore, it may be considered as a universal model to describe the gel strength with reference to concentration.

Table I. Linear Regression Analysis of the Critical Stress - Concentration Relationship With Least Square Method (Apparent viscosity values were included in order to show the variability among the polymers studied)

Polymer type	**Guar gum**	**Lambda Carrageenan (type RLV®)**	**Iota Carrageenan (type VV11PF®)**	**Kappa Carrageenan (type VV71P®)**	**Bentonite RV®**	**Pectin**	**Carbopol 971® NF**
Apparent Viscosity (cP)	400	25	3,400	1,000	4,800	65	185,000
Coefficient α	-32.04	- 0.06	- 63.98	- 19.40	- 4.80	+ 0.03	- 3.41
Sensitivity index	29.10	0.10	40.08	11.55	3.69	0.03	16.26
R^2	0.910	0.961	0.8975	0.9054	0.9503	0.9829	0.9889
Significance	0.022	0.003	0.014	0.048	0.005	0.001	0.001
Polymer type	**Water Lock A-180®**	**Water Lock A-100®**	**Water Lock DD-223®**	**Water Lock G-400®**	**Methocel A4C®**	**Methocel K4M®**	**Na CMC**
Apparent Viscosity (cP)	140,000	36, 000	166, 000	260,000	280	1, 700	2,500
Coefficient α	+ 1.432	- 4.83	+ 4.83	+ 3.76	- 0.61	-5.55	- 4.38
Sensitivity index	4.20	12.99	22.40	12.19	0.48	4.50	6.53
R^2	0.9098	0.9949	0.959	0.9953	0.9369	0.9062	0.9822
Significance	0.012	0.000	0.004	0.000	0.007	0.013	0.001